Dual-light control of nanomachines that integrate motor and modulator subunits

Justin Foy, Quan Li, Antoine Goujon, Jean-Rémy Colard-Itté, Gad Fuks, Emilie Moulin, Olivier Schiffmann, Damien Dattler, Daniel Funeriu, Nicolas Giuseppone

Dual-light control of nanomachines that integrate motor and modulator subunits

Justin T. Foy,[1] Quan Li,[1] Antoine Goujon,[1] Jean-Rémy Colard-Itté,[1] Gad Fuks,[1] Emilie Moulin,[1] Olivier Schiffmann,[2] Damien Dattler,[1] Daniel P. Funeriu,[1] and Nicolas Giuseppone[1]*

[1] SAMS research group, Institut Charles Sadron, University of Strasbourg – CNRS

23 rue du Loess, BP 84047, 67034 Strasbourg Cedex 2, France

[2] Department of Mathematics, UMR CNRS 8628

Bâtiment 425, University Paris-Sud Saclay

91405 Orsay Cedex, France

*e-mail: giuseppone@unistra.fr

A current challenge in the field of artificial molecular machines is the synthesis and implementation of systems that can produce useful work when fueled with a constant source of external energy.[1–5] The first experimental achievements of this kind have consisted of machines with continuous unidirectional rotations[6–14] and translations[15–17] that make use of "Brownian ratchets"[18–25] in order to bias random motions. An intrinsic limitation of such designs is that an inversion of directionality requires heavy chemical modifications in the structure of the actuating motor part.[26,27] Here we show that by connecting subunits made of both unidirectional light-driven rotary motors and modulators, which respectively braid and unbraid polymer chains in crosslinked networks, it becomes possible to reverse their integrated motion at all scales. The photostationary state of the system can be tuned by modulation of frequencies using two irradiation wavelengths. Under this out-of-equilibrium condition, the global work output (*i.e.* contraction or expansion of the material) is controlled by the net flux of clockwise and anticlockwise rotations between the motors and the modulators.

We recently demonstrated the integration and out-of-equilibrium actuation of rotary molecular motors as mechanically active reticulation nodes in polymer networks (Fig. 1a).[28] UV irradiation of such molecular motor/polymer conjugates triggers and sustains the continuous rotation of the motors, producing a subsequent twisting of pairs of polymer chains (i.e. braiding) up to reaching a macroscopic contraction of the entire material. Because the braiding of the polymer chains cannot be reversed without chemical modification of the motor, the resulting twisted conformation is persistent and the process is limited to a

unique contraction event. Access to controlled reversibility is an important issue to address when considering future developments in the field of molecular machines. Indeed, because the intrinsic functioning of individual molecular motors is founded on an asymmetric Brownian ratchet mechanism[18-25] in order to enforce unidirectionality in thermal noise, the reversibility aspect becomes pivotal for systems connecting out-of-equilibrium molecular motors to one another, or to other elements. We now propose a general systemic approach to overcome this limitation. It uses elementary modules made of a combination of two different mechanically active molecular units (Fig. 1b). In this particular network configuration, an elementary module is composed of one rotary motor and one rotary modulator linked by polymer chains. Chemically, the rotary motor is based on a tetra-substituted photoisomerizable crowded alkene[14] (Fig. 1c(*i*)), while the modulator is based on a tetra-substituted dithienylethene photoswitch[29] (Fig. 1c(*ii*)) (see Supplementary Information section 2 for the synthesis and characterization of all compounds). The role of the modulator is to act as an on-demand elastic releaser that operates at a wavelength different from the wavelength that actuates the motor. With UV light, the motor is continuously rotating, while the modulator is in its cyclized form, thus sustaining the torsion of the polymer chains generated by the motor. These combined effects lead to the global contraction of the material. Conversely, when irradiated with visible light, the motor ceases its rotation and the modulator is switched to its open form. The free rotations around C-C single bonds generated can then release the elastic energy accumulated in the braided polymer chains as kinetic energy of rotation until reaching thermodynamic equilibrium. During the process, some energy is also partially dissipated by friction between chains and other irretrievable motions

in the gel. More complex out-of-equilibrium situations may also appear when both the motor and the modulator are concomitantly rotating, thus braiding and unbraiding the polymers with different frequencies.

We first explored a theoretical model of the reversibility at infinite time of such twisted conformation by considering all the possible connections within a large random network (as expected in the gel form). Our mathematical model of the system considers the chemical gel as a random graph embedded in a three-dimensional space. Each vertice is either a motor or a modulator, while edges of the graph are the polymer chains linking them (Figure 2a). The appropriate mathematical model is that of constrained Erdos-Renyi random graphs, and it leads to the following conclusions (see Supplementary Information Section 3 for the full demonstration). (*i*) In the simplest situation, when the system contains an equal number of motors and modulators with each motor linked to a modulator (bipartite graph), the complete unbraiding capacity of the entire network depends only on the number and length of "favorable cycles" in the graph. A "favorable cycle" is defined as a loop containing a series of motors and modulators with at least one motor and one modulator involving "coupled edges" within this loop (see Figure 2a-c for the definition of "coupled edges"). The length l of a favorable cycle is the number of vertices or motors and modulators in the loop. When the total number N of vertices is high, as it is experimentally in the gel, we can precisely determine this number of favorable cycles for each given length and we show that it increases with the power of l. (*ii*) For more complex situations, we have incorporated in our equation the possibility to change the ratio of modulators in the network (let denote $\theta =$ modulator / (motor + modulator)), and to model the efficiency of the unbraiding process by adding two supplementary parameters (γ

and β): γ reflects how more efficient is a shorter cycle compared to a longer one in the unbraiding process, while β measures how more efficient is a cycle containing many active modulators as compared to a cycle containing fewer modulators in the unbraiding process. By taking these parameters as full modeling descriptors of our system, we obtain the following formula:

$$\theta_{crit} = (\frac{\pi}{e^3}\gamma^{-1} - 2 - e^{-\beta})(e^{\beta} - e^{-\beta})^{-1}$$

In other words, at the asymptotic limit $N \to \infty$, the polymer network is fully uncoiling if $\theta \geq \theta_{crit}$. For instance, and for one of the less favorable situations (γ = 0.06, β = 2), a concentration of only 5% in open modulator is sufficient to fully unbraid the system once the motor is stopped (see plotted equation in Supplementary Information).

Further, a molecular study of the modulator subunit proved its kinetic efficiency of rotation and thus its potential as an elastic releaser. Dithienylethene tetra-benzylic alcohol $\mathbf{1}^{\mathbf{open}}$ was first synthesized in 8 steps from commercially available products, and its structure was confirmed by X-ray crystallography (Figure 3a,b) (see also Supplementary Information Sections 2 and 4). $\mathbf{1}^{\mathbf{open}}$ exists as a mixture of two conformers (parallel and antiparallel) with a ratio of 77:23 in acetonitrile as determined by ^{1}H NMR (see Supplementary Information Section 5). Photocyclisation of $\mathbf{1}^{\mathbf{open}}$ into $\mathbf{1}^{\mathbf{closed}}$ is achieved by irradiation with UV light, while the reverse process is performed by irradiation with visible light. The ring closure is confirmed by the appearance of a characteristic purple color with a maximum absorption band at 530 nm during UV irradiation; and the ring opening is confirmed by the color disappearance when using visible light (Fig. 3c). At the photostationnary state with UV light, ^{1}H NMR reveals a ratio $\mathbf{1}^{\mathbf{open}}$:$\mathbf{1}^{\mathbf{closed}}$ of 60:40

([**1**] = 1.5 10^{-4} M in CD_3CN). Despite a more important steric hindrance, a similar behavior was found for tetra-subsituted dithienylethene **2** which incorporates four tetra-ethylene glycol arms terminated with azide functions, the actual synthon integrated further in the gel network. For **1** and **2**, the possibility to discriminate the parallel and antiparallel conformations by ^1H NMR is the consequence of a barrier of rotation between the two conformers. We determined activation energy values of 73 kJ.mol^{-1} for **1** and 72 kJ.mol^{-1} for **2** by variable temperature experiments (see Supplementary Information Section 6). One can thus conclude that the open modulators of this study interconvert in solution and at room temperature with experimentally determined frequencies of 1.0 Hz for **1** and of 1.5 Hz for **2**. We also plotted the energy profile of the tetra-methoxy derivative of $\mathbf{1}^{\mathbf{open}}$ for a 360° rotation of the C_4-C_{27} bond as determined by density functional theory (DFT) (Fig. 3d and Supplementary Information section 7). We found two close transition states **TS1** (63.2 kJ.mol^{-1}) and **TS2** (66.7 kJ.mol^{-1}), confirming a full and easy rotation at room temperature with a frequency of 10.1 Hz. This higher rotation rate compared to **1** and **2** is explained by the absence of internal hydrogen bonds or bulky substituents in the molecular model, and confirms the possibility for the modulator to perform its role as a conformational disentangler by full rotation when connected in the chemical gel.

With these preliminary elements in hand, we chemically linked the motor and modulator subunits in different proportions within cross-linked gels (Fig. 4a). A first reference **Gel 0** (containing 0 mol% of modulator) was obtained by reacting one equivalent of enantiopure motor tetra-alkyne **3** with one equivalent of motor tetra-azide **4** by a copper-catalyzed Huisgen[3+2] cycloaddition ('click reaction') (see Supplementary Information Section 9 for the choice of working in

enantiopure series). At the opposite, **Gel 50** (containing 50 mol% of modulator) was obtained using the same reaction conditions but by mixing one equivalent of motor tetra-alkyne **3** with one equivalent of modulator tetra-azide **2**. Gels of intermediate compositions (**Gels 25, 12, 5**) were also synthesized following the percentages of the chart shown in Fig. 4a. By performing the 'click' reaction directly in metallic molds of fixed volumes, transparent gels were obtained with thicknesses comprised between 476 μm and 2 mm, and with a surface comprised between 2 and 4 cm^2 (Fig. 4a). We first investigated a set of contraction experiments on **Gel 50** swollen in acetonitrile and noticed that the absorption of dithienylethene was important and that UV light cannot penetrate the entire volume of the sample for a thickness above 1 mm (see Supplementary Figure 5). We thus studied the contraction of the series **Gel 0-50** for a thickness of 476 μm. All the five gels significantly contracted as shown by the variations of volume as a function of time (Fig. 4b). As the percentage of modulator was decreased, we observed a higher speed of contraction at initial time and a higher maximal percentage of contraction at steady state. Moreover, for high amounts of modulator (**Gel 50**) an observable activation period is taking place at the early irradiation times. This is likely the signature of a cooperative effect: as the motor is pulling on the polymer chains, the antiparallel / parallel ratio of the modulator is increasing, leading to a different photostationary state more biased in favor of the closed form. This amplification of the bias is much less pronounced for lower percentage of modulator (**Gel 25**) and, for **Gel 5**, the initial rate of the contraction (V_0 = 63 vol%.h^{-1}; corresponding to an apparent frequency of the motor F_{app}^{cont}= 31.7 10^{-3} Hz) is close to the one observed for reference **Gel 0** (V_0 = 84 vol%.h^{-1}; F_{app}^{cont} = 42.2 10^{-3} Hz) (see Supplementary Information Section 8 for the

determination of the apparent frequencies in the gel state). As expected, when switching off the UV lamp and exposing the sample to white light, all gels went back close to their initial volume within tens of hours at room temperature, except non-reversible **Gel 0** which maintained its full contraction (Fig. 4c). The expansion of the gels is the result of two parameters: the elasticity of the braided polymer network and the osmotic pressure generated by the solvation of the polymer chains. The solvent, after expulsion during the contraction (syneresis), participates to the reversibility of the process by swelling the gel. Indeed, a visible irradiation of the contracted gel in the dry state did not show expansion. In another control experiment under proper swelling conditions, the UV light was turned off after full contraction of **Gel 50**. We measured a complete but slower expansion in the dark (F_{app}^{exp} = 1.7 10^{-4} Hz) compared to the expansion under visible light (F_{app}^{exp} = 4.8 10^{-4} Hz), indicating that the percentage of efficient open modulators is indeed lower without specific activation of the photochemical switch. The decrease of modulator percentage in the gel also moderately affects its rate of expansion, with apparent frequencies comprised within 4.8 10^{-3} Hz for **Gel 50** and 1.3 10^{-3} Hz for **Gel 12**. These experiments indicate that small ratios of modulators/motors can be used, as suggested by our mathematical model. This decrease of modulator concentration allows for an improved work output of the system, namely a faster kinetic response and a higher maximal contraction at steady state.

Finally, in order to regulate the contraction of a 1 mm thick **Gel 50**, we performed a dual light control experiment involving constant UV irradiation (continuous rotation of the motor), while varying at the same time the quantity of open modulator with a white light emitting diode (LED, 30 lm) placed at variable

distances from the sample (Fig. 4d). By finding an appropriate regime between the intensities of the UV lamp and the LED, we confirmed that one can finely tune at steady state the contraction of the gel depending on the intensity delivered by the LED (being here regulated by the distance between the source and the sample). This key observation shows that the work produced by the system at the photostationary state is the result of a net flux of rotations at nanoscale between the motors and the modulators turning in opposite directions.

The results reported here show the fully out-of-equilibrium control of artificial molecular machine-based materials. The basic concept rests on connecting a nanomotor to a releasing elementary unit (that functions as a clutch) within modules that are functionally robust against thermal noise. This systemic approach provides a general solution to overcome the unidirectionality limitation associated with the necessary use of Brownian ratchets when working out-of-equilibrium at nanoscale. Because the individual units of the module can be actuated at two different wavelengths, the work output at steady state can be finely tuned by modulation of frequencies. In order to produce a useful work with such systems, the only constraint is that the apparent frequency of the motor has to be set higher than the apparent frequency of the modulator (see Supplementary Information Section 9). This new kind of artificial materials stimulates the necessary transition engaged by chemists from the control over individual molecular motors towards the design of more complex nanomachines integrating different operating units that work in concert. Here the reversibility process relies on the elasticity of the polymer system and on osmotic pressure, as for example it is the case in biology with cytoskeleton and titin proteins resetting the sarcomere units in muscles.[30] Further, by using these general out-of-equilibrium principles

that are reminiscent of life-like materials,[31,32] one can imagine a plethora of artificial systems in order to convert energies and to modulate functions at all scales.

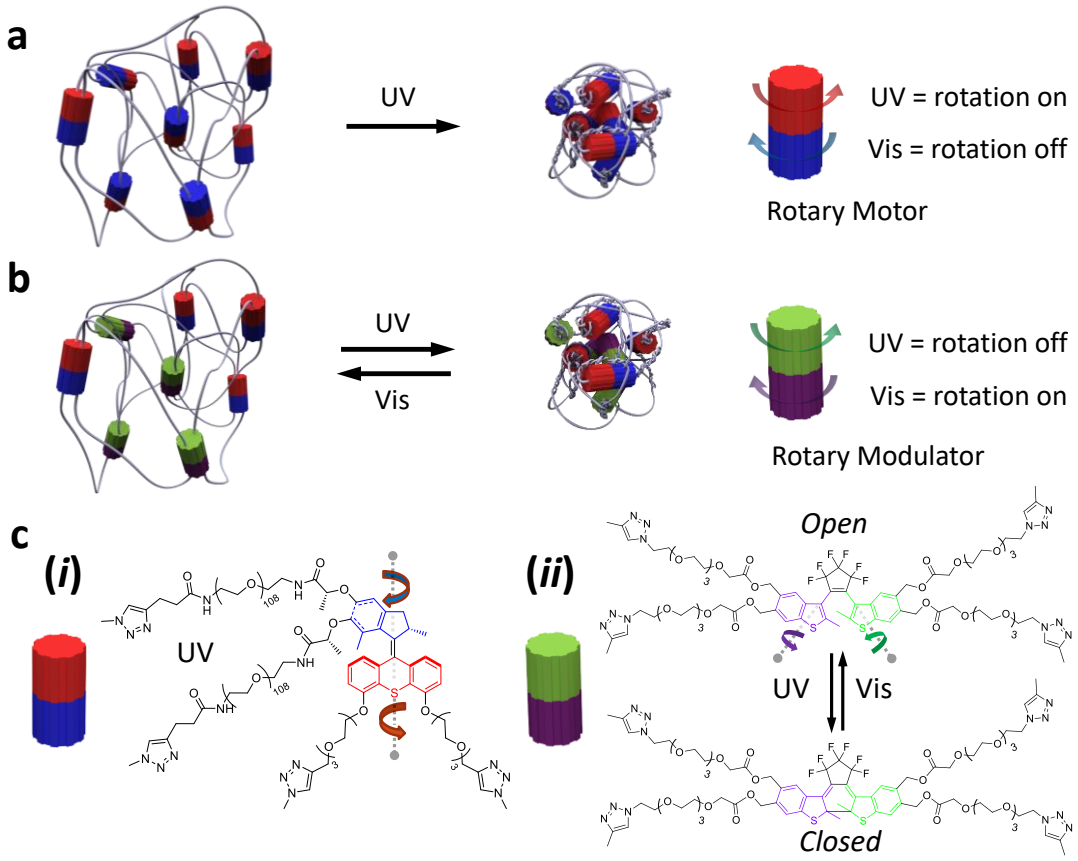

Figure 1 | Functioning principle and chemical design of an integrated motor/modulator system. a, Schematic representation of a reticulated polymer-motor gel which, under UV light irradiation, produces a continuous unidirectional out-of-equilibrium rotation of the motor part (red and blue cylinders) with the subsequent braiding of the polymer chains, leading to a macroscopic contraction of the entire network. A braid is defined as a twisted pair of polymer chains. **b,** Schematic representation of a polymer-motor-modulator gel which proceeds as in (**a**) when exposed to UV light, but which unbraids the polymer chains when exposed to Vis light by activating the modulator part (green and purple cylinders). Visible light-activation of the modulator allows its rotation in the opposite direction of the elastic torque initially produced by the motor, thus leading to a full re-expansion of the network at thermodynamic equilibrium. **c,** Chemical structures composing the polymer-motor-modulator system studied herein, involving enantiopure crowded alkenes as motors (***i***) and photoswitchable dithienylethenes as modulators (***ii***). Under UV irradiation, the motor is continuously rotating in one direction while the modulator is locked in its closed form. Conversely, under Vis light irradiation, the motor is stopped and the modulator is switched to its open form that liberates two freely rotating single bonds that can unbraid the adjacent polymer chains.

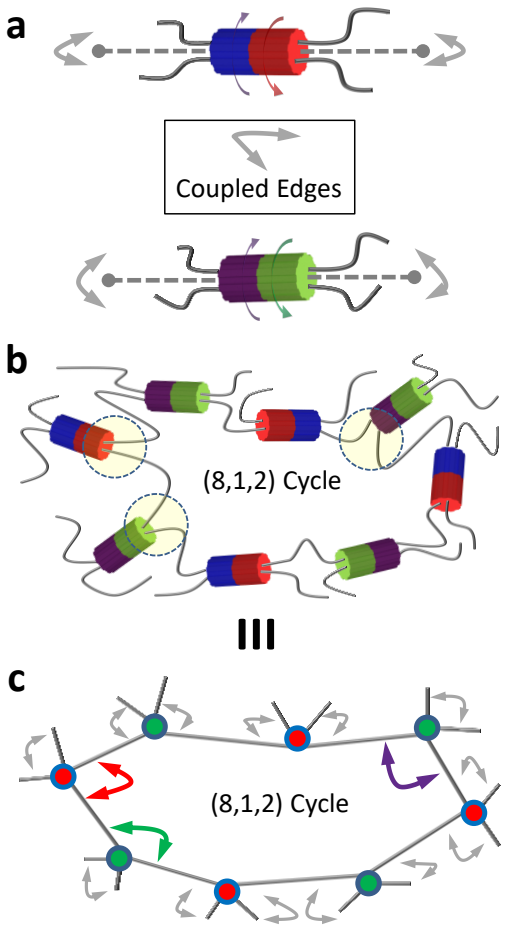

Figure 2 | Schematic representations of the mechanical topology acting in the gel. a, In this simplest example, a random bipartite graph is used to model the polymer-motor-modulator system: it is composed of 50% motors and 50% modulators as vertices, and of polymer chains as edges. “Coupled edges” are defined by two polymer chains attached to the same side of a given motor/modulator. A coupled edge corresponds to the two chains that will be braided by a single motor; or to the two chains in a braid that will be unwound by a modulator. Note that in a bipartite graph, each motor is linked to a modulator. **b,** Schematic representation of a (8,1,2) cycle of length 8 (8 vertices), and containing 1 motor and 2 modulators with coupled edges within this cycle (see circled connections). The chemical topology of this particular cycle is favorable for both braiding (due to the coupled edges motor) and unbraiding (due to the two coupled edges modulators). **c,** Mathematical graph encoding the cycle represented in (**b**).

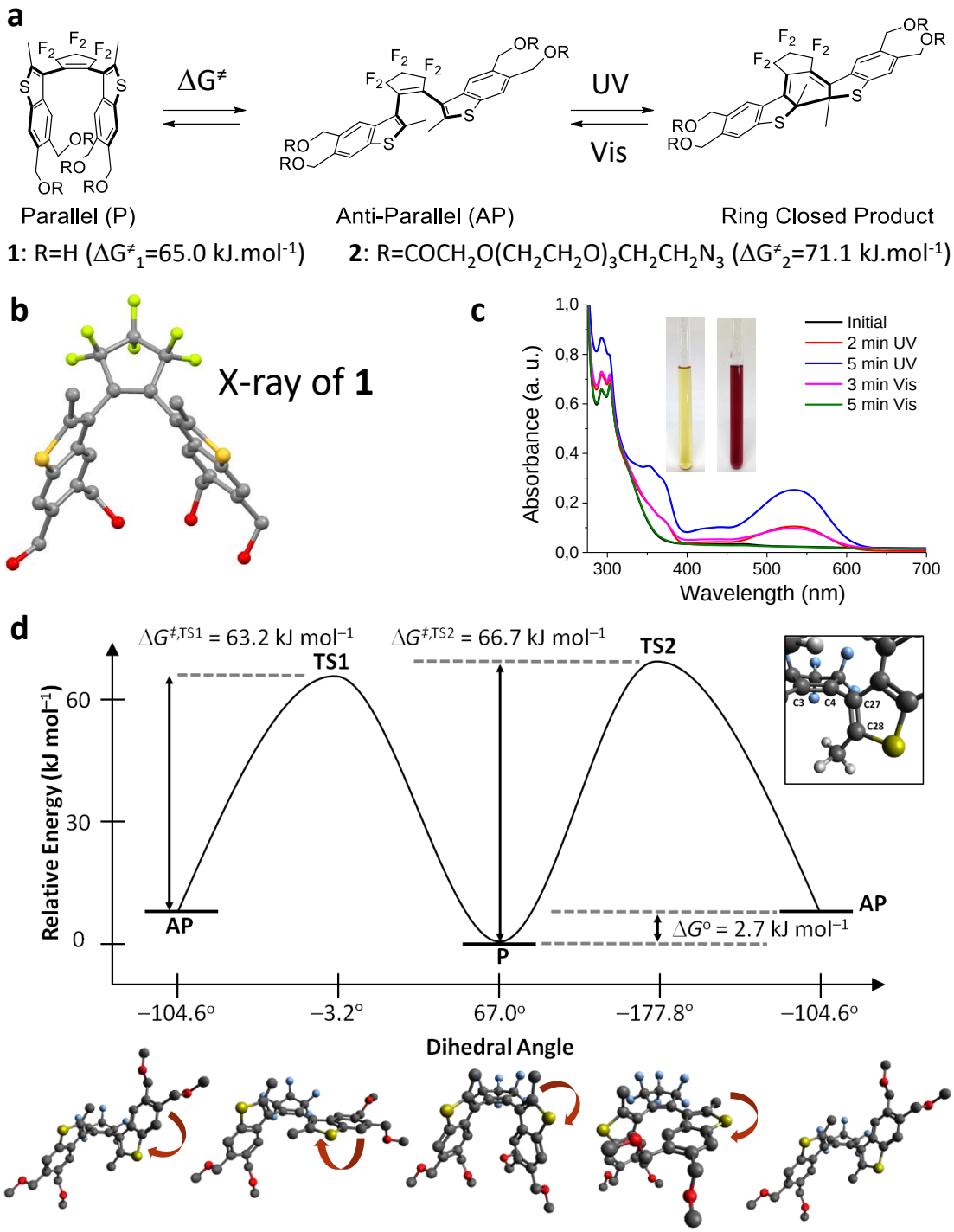

Figure 3 | Rotational dynamics in individual modulator subunits. a, Dithienylethenes are engaged in coupled equilibria when submitted to a UV irradiation. The first one occurs between a parallel and an anti-parallel open form by rotation of two C-C single bonds. This rotation is associated to the activation energy ($\Delta G^{\neq}$) that determines the frequency of rotation at a given temperature (and which also depends on the bulkiness of the R substituents). The experimental values of $\Delta G^{\neq}$ for **1** and **2** were determined by variable temperature ^{1}H NMR experiments. The

second one occurs between the anti-parallel open form and the ring closed form, with a given distribution of each form at the photostationary state which can also be determined by ^{1}H NMR (see Supporting Information section 5). **b,** Crystal structure of **1** in its open parallel form. **c,** UV-Vis absorption spectra of **1** in solution (c = 1.5 10^{-4} M in CH_3CN) after different times of irradiation with UV and Visible light; the absorption at 530 nm is characteristic of the closed form and is resulting in a purple color of the solution. **d,** Energy profile determined by DFT calculations for a full rotation (360°) of the thiophene unit around the C_4-C_{27} single bond connected to the cyclopentene moiety. The calculation is performed on the tetra-methoxy derivative of dithienylethene **1** in order to avoid the presence of intramolecular hydrogen bonds. The highest $\Delta G^{\neq}$ value corresponds to the interaction between the left methyl and the right aromatic ring of the dithienylethene (TS2).

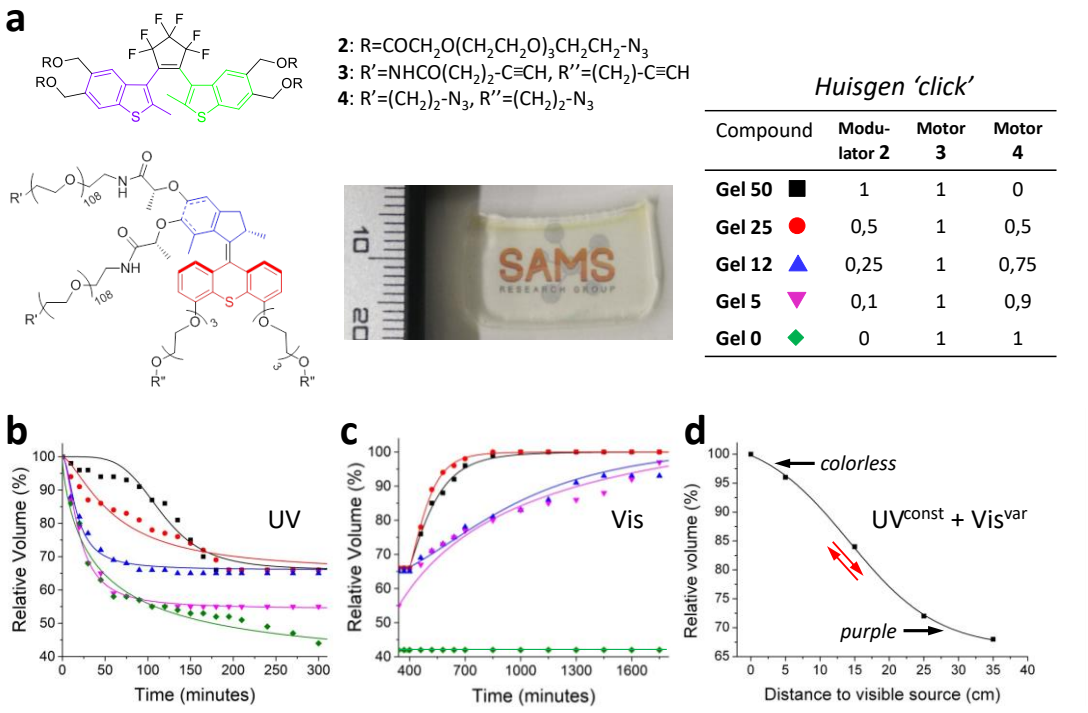

Figure 4 | Actuation at two wavelengths of integrated motor/modulator systems. a, Chemical structures, compositions, and labels of various gels obtained by 'click' cyclization catalyzed by Cu(I), depending on their content in motors **3** and **4** (100-50 mol%) and modulator **2** (0-50 mol%). The photography shows a transparent piece of **Gel 5** (1 cm X 2 cm X 0.2 cm). **b,** Relative volume contraction ($(V_{(t=0)} - V_{(t)})/V_{(t=0)}$) as a function of time for **Gels 0-50** (initial thickness of 476 μm) that have various contents of modulator. The lines guide the eye through the trends. **c,** Relative volume expansion as a function of time for **Gel 0-50** that have various contents of modulator and starting from the photostationary state reached in (**b**). The lines guide the eye through the trends. **d**, Dual-light control of **Gel 50** (thickness = 1 mm) under constant UV irradiation (UV^{const} at a fixed distance of 6 cm from the gel) and by varying the intensity of a second and concomitant irradiation with a white LED of 30 lm (Vis^{var} with the x axis representing the distance between the white LED and the sample). Each point is measured at steady state and the system can be tuned in both directions (red arrows). When the LED is close enough, the gel is colorless and expanded (open modulator), while at longer distances, the gel becomes purple and contracts (closed modulator). The lines guide the eye through the trends.

Acknowledgements

The research leading to these results has received funding from the European Research Council under the European Community's Seventh Framework Program (FP7/2007-2013) / ERC Starting Grant agreement n°257099 (N.G.). We thank ANR (project INTEGRATIONS) for financial support. We also wish to thank the Centre National de la Recherche Scientifique (CNRS), the COST action (CM 1304), the international center for Frontier Research in Chemistry (icFRC), the Laboratory of Excellence for Complex System Chemistry (LabEx CSC), the University of Strasbourg (UdS), and the Institut Universitaire de France (IUF). Q.L. thanks the China Scholarship Council (CSC) for a doctoral fellowship. We are grateful to Gérard Strub for manufacturing the molds to shape the gels, Julie Lemoine for HPLC purifications, and J.-M. Strub for HRMS. The authors also thank Dr. Vincent Le Houerou for discussions.

Author Contributions

G.F., E.M., and N.G. conceived the work. J.F., Q.L., A.G., J.-R.C.-I. and D.D. performed the experiments. O.S. established the mathematical model. All authors discussed and interpreted the data. N.G. wrote the paper with all authors commenting on the manuscript.

Additional Information

Supplementary information is available in the online version of the paper. Reprints and permission information is available online at http://npg.nature.com/reprints. Correspondence and requests for materials should be addressed to N.G.

Competing Financial Interests

The authors declare no competing financial interests.

References

1. Abendroth, J. M., Bushuyev, O. S., Weiss, P. S. & Barrett, C. J. Controlling Motion at the Nanoscale: Rise of the Molecular Machines. *ACS Nano* **9,** 7746–7768 (2015).

2. Erbas-Cakmak, S., Leigh, D. A., McTernan, C. T. & Nussbaumer, A. L. Artificial Molecular Machines. *Chem. Rev.* **115,** 10081–10206 (2015).

3. Coskun, A., Banaszak, M., Astumian, R. D., Stoddart, J. F. & Grzybowski, B. A. Great expectations: can artificial molecular machines deliver on their promise? *Chem. Soc. Rev.* **41,** 19–30 (2012).

4. Browne, W. R. & Feringa, B. L. Making molecular machines work. *Nat. Nanotechnol.* **1,** 25–35 (2006).

5. Kinbara, K. & Aida, T. Toward Intelligent Molecular Machines: Directed Motions of Biological and Artificial Molecules and Assemblies. *Chem. Rev.* **105,** 1377–1400 (2005).

6. Kistemaker, J. C. M., Štacko, P., Visser, J. & Feringa, B. L. Unidirectional rotary motion in achiral molecular motors. *Nat. Chem.* **7,** 890–896 (2015).

7. Greb, L., Eichhöfer, A. & Lehn, J.-M. Synthetic Molecular Motors: Thermal N Inversion and Directional Photoinduced C=N Bond Rotation of Camphorquinone Imines. *Angew. Chem. Int. Ed.* **54,** 14345–14348 (2015).

8. Guentner, M. *et al.* Sunlight-powered kHz rotation of a hemithioindigo-based molecular motor. *Nat. Commun.* **6,** 8406 (2015).

9. Greb, L. & Lehn, J.-M. Light-Driven Molecular Motors: Imines as Four-Step or Two-Step Unidirectional Rotors. *J. Am. Chem. Soc.* **136,** 13114–13117 (2014).

10. Wang, J. & Feringa, B. L. Dynamic Control of Chiral Space in a Catalytic Asymmetric Reaction Using a Molecular Motor. *Science* **331,** 1429–1432 (2011).

11. Kudernac, T. *et al.* Electrically driven directional motion of a four-wheeled molecule on a metal surface. *Nature* **479,** 208–211 (2011).

12. Klok, M. *et al.* MHz Unidirectional Rotation of Molecular Rotary Motors. *J. Am. Chem. Soc.* **130,** 10484–10485 (2008).

13. Eelkema, R. *et al.* Molecular machines: Nanomotor rotates microscale objects. *Nature* **440,** 163 (2006).

14. Koumura, N., Zijlstra, R. W. J., van Delden, R. A., Harada, N. & Feringa, B. L. Light-driven monodirectional molecular rotor. *Nature* **401,** 152–155 (1999).

15. Ragazzon, G., Baroncini, M., Silvi, S., Venturi, M. & Credi, A. Light-powered autonomous and directional molecular motion of a dissipative self-assembling system. *Nat. Nanotechnol.* **10,** 70–75 (2015).

16. Cheng, C. *et al.* An artificial molecular pump. *Nat. Nanotechnol.* **10,** 547–553 (2015).

17. Balzani, V. *et al.* Autonomous artificial nanomotor powered by sunlight. *Proc. Natl. Acad. Sci.* **103 ,** 1178–1183 (2006).

18. Cheng, C., McGonigal, P. R., Stoddart, J. F. & Astumian, R. D. Design and Synthesis of Nonequilibrium Systems. *ACS Nano* **9,** 8672–8688 (2015).

19. Astumian, R. D. Microscopic reversibility as the organizing principle of molecular machines. *Nat. Nanotechnol.* **7,** 684–688 (2012).

20. Serreli, V., Lee, C.-F., Kay, E. R. & Leigh, D. A. A molecular information ratchet. *Nature* **445,** 523–527 (2007).

21. Astumian, R. D. Design principles for Brownian molecular machines: how to swim in molasses and walk in a hurricane. *Phys. Chem. Chem. Phys.* **9,** 5067–5083 (2007).

22. Chatterjee, M. N., Kay, E. R. & Leigh, D. A. Beyond Switches: Ratcheting a Particle Energetically Uphill with a Compartmentalized Molecular Machine. *J. Am. Chem. Soc.* **128,** 4058–4073 (2006).

23. Mahadevan, L. Motility Powered by Supramolecular Springs and Ratchets. *Science* **288,** 95–99 (2000).

24. Astumian, R. D. Thermodynamics and Kinetics of a Brownian Motor. *Science* **276,** 917–922 (1997).

25. Peskin, C. S., Odell, G. M. & Oster, G. F. Cellular motions and thermal fluctuations: the Brownian ratchet. *Biophys. J.* **65,** 316–324 (1993).

26. Ruangsupapichat, N., Pollard, M. M., Harutyunyan, S. R. & Feringa, B. L. Reversing the direction in a light-driven rotary molecular motor. *Nat. Chem.* **3,** 53–60 (2011).

27. Fletcher, S. P., Dumur, F., Pollard, M. M. & Feringa, B. L. A Reversible, Unidirectional Molecular Rotary Motor Driven by Chemical Energy. *Science* **310 ,** 80–82 (2005).

28. Li, Q. *et al.* Macroscopic contraction of a gel induced by the integrated motion of light-driven molecular motors. *Nat. Nanotechnol.* **10,** 161–165 (2015).

29. Irie, M., Fukaminato, T., Matsuda, K. & Kobatake, S. Photochromism of Diarylethene Molecules and Crystals: Memories, Switches, and Actuators. *Chem. Rev.* **114,** 12174–12277 (2014).

30. Maughan, D. W. & Godt, R. E. A quantitative analysis of elastic, entropic, electrostatic, and osmotic forces within relaxed skinned muscle fibers. *Biophys. Struct. Mech.* **7,** 17–40 (1980).

31. Boekhoven, J., Hendriksen, W. E., Koper, G. J. M., Eelkema, R. & van Esch, J. H. Transient assembly of active materials fueled by a chemical reaction. *Science* **349,** 1075 – 1079 (2015).

32. Grzybowski, B. A. & Huck, W. T. S. The nanotechnology of life-inspired systems. *Nat. Nanotechnol.* **11,** 585–592 (2016).